

## Supporting Information

### **The Role of Anions on Light-Driven Conductivity in Diarylethene-Containing Polymeric Ionic Liquids**

Hui Nie,<sup>a‡</sup> Nicole S. Schausser,<sup>b‡</sup> Neil D. Dolinski,<sup>b†</sup> Zhishuai Geng,<sup>b</sup> Saejin Oh,<sup>a</sup> Michael L. Chabinyc,<sup>b</sup> Craig J. Hawker,<sup>ab</sup> Rachel A. Segalman,<sup>bc\*</sup> Javier Read de Alaniz<sup>a\*</sup>

<sup>a</sup>Department of Chemistry and Biochemistry, University of California–Santa Barbara, Santa Barbara, CA 93106, USA

<sup>b</sup>Materials Department and Materials Research Laboratory, University of California–Santa Barbara, Santa Barbara, CA 93106, USA

<sup>c</sup>Department of Chemical Engineering, University of California–Santa Barbara, Santa Barbara, CA 93106, USA

## Table of Contents

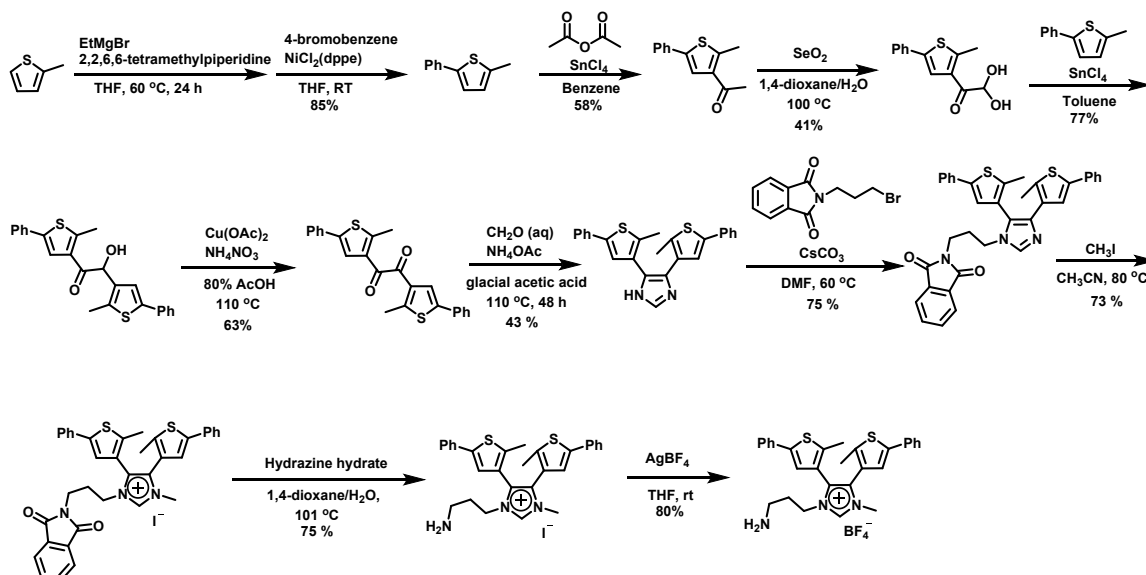
<b>Materials and methods .....</b>	<b>3</b>
<b>Synthesis of PEO-<i>stat</i>-PAGE-DAE-X (X=I, BF<sub>4</sub>, TFSI) .....</b>	<b>4</b>
<b><i>T<sub>g</sub></i>s of PEO-<i>stat</i>-PAGE-DAE-X (X=I, BF<sub>4</sub>, TFSI) .....</b>	<b>5</b>
<b><sup>1</sup>H NMR of PEO-<i>stat</i>-PAGE-DAE-X (X=I, BF<sub>4</sub>, TFSI) .....</b>	<b>6</b>
<b><sup>1</sup>H NMR of phthalimide protected DAE-I with UV light irradiation .....</b>	<b>7</b>
<b>Pump probe measurements and calculations of DAE-X and PEO-<i>stat</i>-PAGE-DAE-X .....</b>	<b>8</b>
<b>Ionic conductivity measurements .....</b>	<b>16</b>
<b><i>T<sub>g</sub></i>s of PEO-<i>stat</i>-PAGE-DAE-BF<sub>4</sub> before and after irradiation .....</b>	<b>20</b>
<b><sup>1</sup>H NMR and <sup>13</sup>C NMR spectra .....</b>	<b>21</b>
<b>References .....</b>	<b>25</b>

## Materials and methods

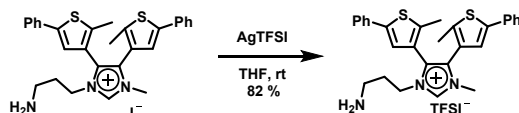
Unless otherwise specified, reagents were purchased from commercial sources and used without further purification. Flash column chromatography was performed with Merck silica gel 60 (70-230 mesh). All chromatographic solvents were of ACS grade and used without further purification. Analytical thin-layer chromatography (TLC) was carried out with Merck silica gel 60 F254 glass plates and visualized using UV lamp.  $^1\text{H}$  and  $^{13}\text{C}$  NMR spectroscopy were recorded on a Varian VNMRs 600 (600 MHz for  $^1\text{H}$  and 150 MHz for  $^{13}\text{C}$ ) spectrometer, Varian Inova-500 (500 MHz for  $^1\text{H}$ , and 125 MHz for  $^{13}\text{C}$ ). Chemical shifts are reported relative to residual solvent peaks ( $\delta$  7.26 for  $\text{CDCl}_3$  in  $^1\text{H}$  NMR and  $\delta$  77.2 for  $\text{CDCl}_3$  in  $^{13}\text{C}$  NMR;  $\delta$  5.32 for  $\text{CD}_2\text{Cl}_2$  in  $^1\text{H}$  NMR and  $\delta$  53.8 for  $\text{CD}_2\text{Cl}_2$  in  $^{13}\text{C}$  NMR). FTIR spectra were recorded on a Perkin Elmer Spectrum 2 FT/IR or a Perkin Elmer Spectrum 100 employing a Universal ATR Sampling Accessory and are reported in terms of frequency of absorption ( $\text{cm}^{-1}$ ). Mass spectral data were collected on a Micromass QTOF2 Quadrupole/Time-of-Flight Tandem mass spectrometer (ESI-MS). Details for pump-probe UV-vis absorption and photoswitching measurements are presented in the respective sections. UV-Vis absorption spectra were recorded on Agilent 8453 UV-vis spectrometer. Polymer samples were fully dried under vacuum and characterized with a TA Instruments Q2000 DSC to measure the glass transition temperature ( $T_g$ ) on second heating at  $20\text{ }^\circ\text{C min}^{-1}$ .

## Synthesis of PEO-*stat*-PAGE-DAE-X (X=I, BF<sub>4</sub>, TFSI)

1-(3-aminopropyl)-3-methyl-4,5-bis(2-methyl-5-phenylthiophen-3-yl)-1H-imidazol-3-ium iodide and 1-(3-aminopropyl)-3-methyl-4,5-bis(2-methyl-5-phenylthiophen-3-yl)-1H-imidazol-3-ium tetrafluoroborate were synthesized according to the following reported procedures.<sup>1</sup>



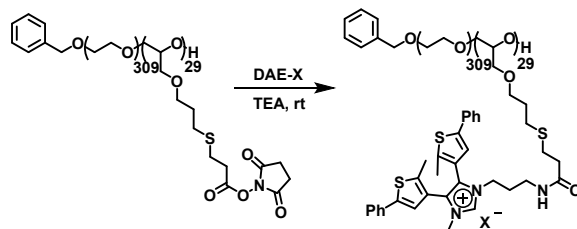
Synthesis of 1-(3-aminopropyl)-3-methyl-4,5-bis(2-methyl-5-phenylthiophen-3-yl)-1H-imidazol-3-ium bis(trifluoromethanesulfonyl)imide (DAE-TFSI)



A 20 mL vial equipped with a stir bar was charged with 230 mg (0.376 mmol) of 1-(3-aminopropyl)-3-methyl-4,5-bis(2-methyl-5-phenylthiophen-3-yl)-1H-imidazol-3-ium iodide dissolved in 10 mL of mixture of MeOH and THF. To the vial was added 146 mg (0.376 mmol) of silver bis(trifluoromethanesulfonyl)imide dissolved in 2 mL of MeOH. A white precipitate formed immediately, and the reaction was stirred at room temperature for a further 15 min. The mixture was then filtered and the filtrate was concentrated and dried under reduced pressure to yield the desired product as a powder. <sup>1</sup>H NMR (500 MHz, Chloroform-d) δ 9.16 (s, 1H), 7.53 (m, 4H), 7.38 (m, 4H), 7.30 (m, 2H), 7.22 (s, 2H), 4.25 (m, 2H), 3.83 (s, 3H), 2.77 (t, 2H), 2.30 (s, 3H), 2.09 (s, 3H), 1.94(m, 2H). <sup>13</sup>C NMR (125 MHz, Chloroform-d) δ 143.14, 142.97, 141.88, 136.92, 133.02, 132.98, 129.08, 129.06, 128.78, 128.16, 128.10, 127.84, 125.54, 125.52, 123.64, 123.03, 122.04, 121.09, 118.53, 45.74, 38.01, 34.72, 31.81, 13.92, 13.85. IR (ATR) 3158, 3090, 2931, 2852, 1571, 1447, 1347, 1325, 1176, 1132, 1050, 756, 688, 648, 596, 569 cm<sup>-1</sup>. HRMS Positive ion mode (ESI) m/z 484.1881, calc. 484.1877 for [DAE]<sup>+</sup>. Negative ion mode (ESI) m/z 279.9170, calc. 279.9173 for [TFSI]<sup>-</sup>.

### Synthesis of polymerized ionic liquid (PIL) PEO-*stat*-PAGE-DAE-X (X=I, BF<sub>4</sub>, TFSI)

The PEO-*stat*-PAGE polymer with ~10 mol% of AGE units and molecular weight of 17 k ( $M_n$ ) was synthesized according to a procedure described by Lee et al.<sup>2</sup> Synthesis of 3-Mercaptopropanyl-N-hydroxysuccinimide Ester functionalized PEO-*stat*-PAGE polymer was carried out according to reported procedures.<sup>1</sup>



To a solution of DAE-I (160 mg, 0.26 mmol) or DAE-BF<sub>4</sub> (150 mg, 0.26 mmol) or DAE-TFSI (200 mg, 0.26 mmol) and triethylamine (100  $\mu$ L) in dry CH<sub>2</sub>Cl<sub>2</sub> (15 mL), 3-Mercaptopropanyl-N-hydroxysuccinimide Ester functionalized PEO-*stat*-PAGE (26 mg, about 0.043 mmol) in CH<sub>2</sub>Cl<sub>2</sub> (about 2 mL) was added. The solution was stirred for around 24 h at room temperature, then CH<sub>2</sub>Cl<sub>2</sub> was dried under vacuum. Methanol and small amount of CH<sub>2</sub>Cl<sub>2</sub> were added to dissolve the solid residue with sonication. The obtained solution was subjected to dialysis in methanol for 2 days for purification.

### $T_g$ s of PEO-*stat*-PAGE-DAE-X (X=I, BF<sub>4</sub>, TFSI)

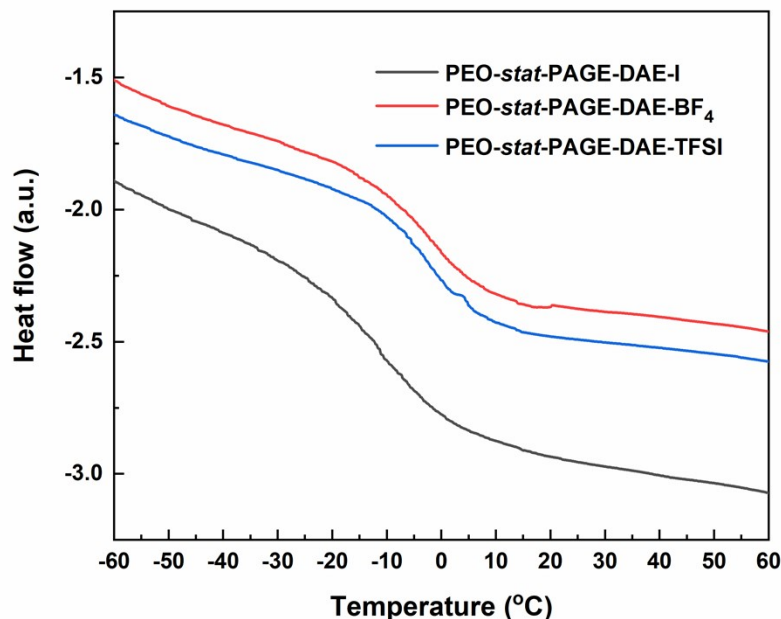


Figure S1.  $T_g$  of PEO-*stat*-PAGE-DAE-X (I, BF<sub>4</sub>, TFSI).

**<sup>1</sup>H NMR of PEO-*stat*-PAGE-DAE-X (X=I, BF<sub>4</sub>, TFSI)**

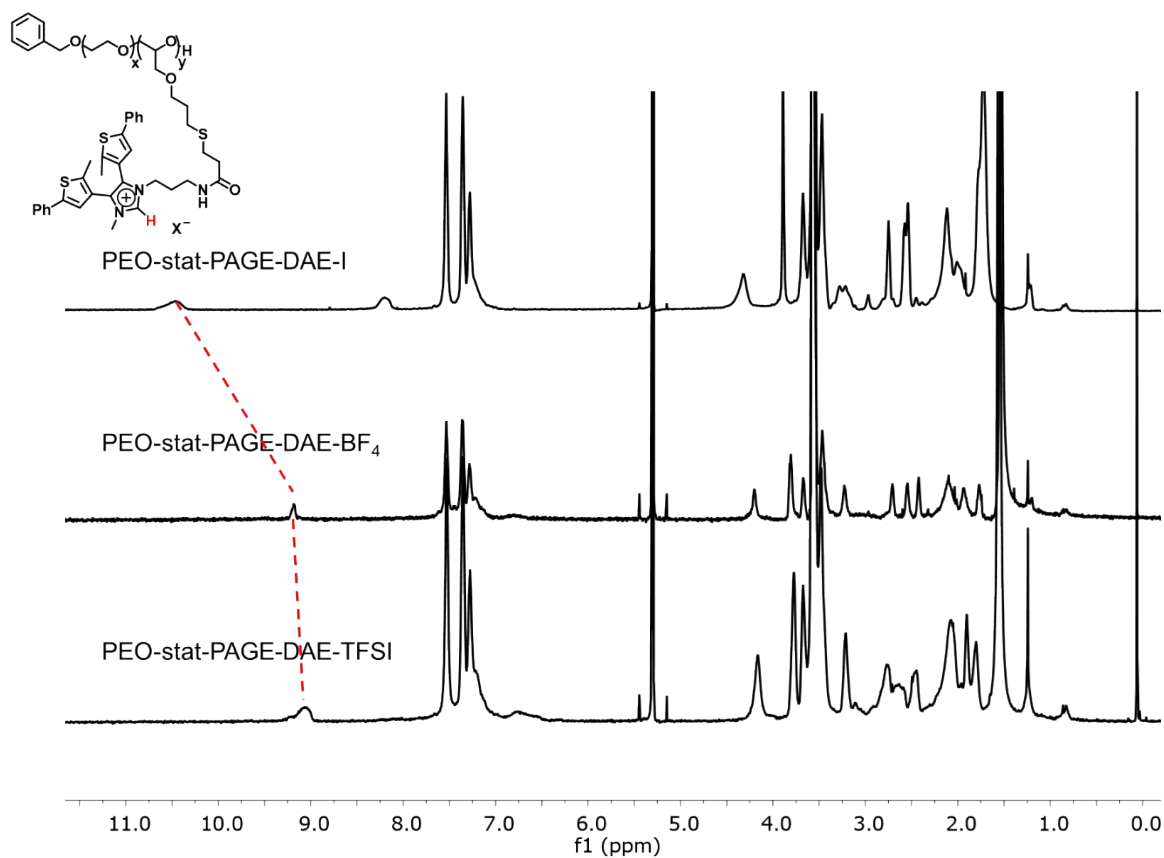


Figure S2. <sup>1</sup>H NMR of PEO-*stat*-PAGE-DAE-X (I, BF<sub>4</sub>, TFSI) in CD<sub>2</sub>Cl<sub>2</sub>, and the high field chemical shift of C2 proton indicating weaker cation-anion interactions.

### <sup>1</sup>H NMR of phthalimide protected DAE-I with UV light irradiation

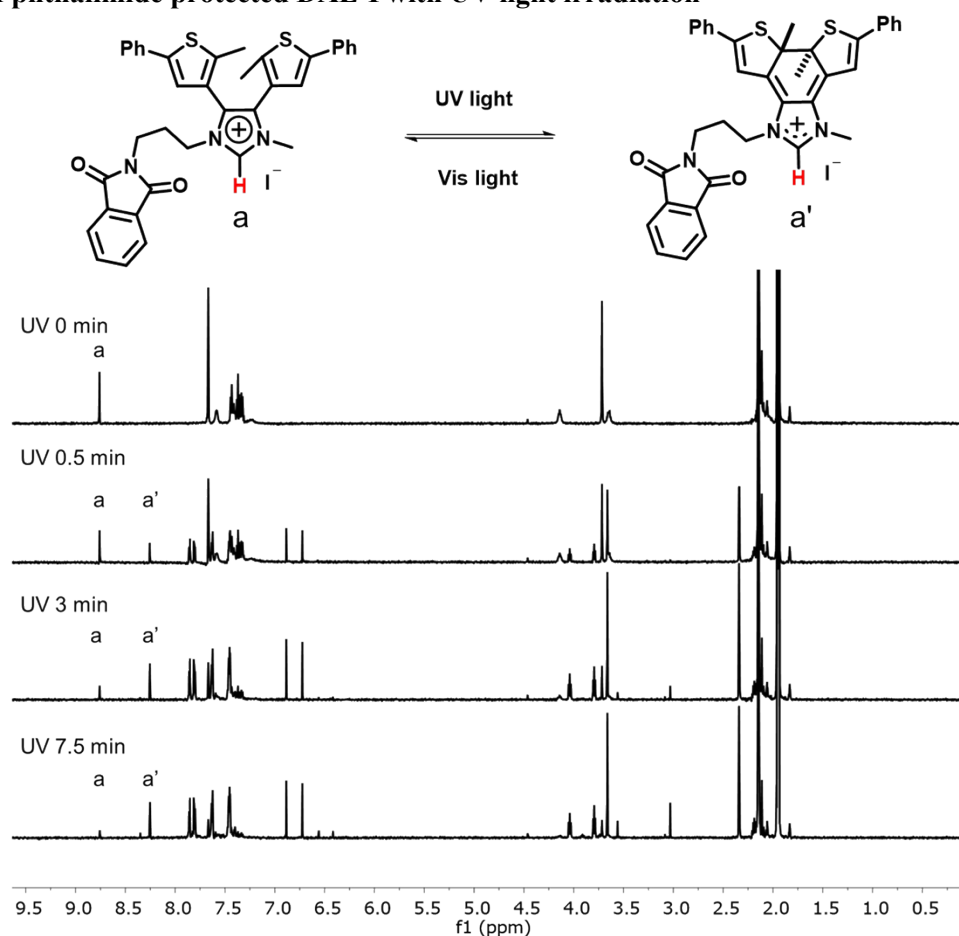


Figure S3. <sup>1</sup>H NMR spectra of the phthalimide protected DAE-I with 300 nm light irradiation in CD<sub>3</sub>CN. The light source used here is Rayonet Photochemical reactor with 3000 Å lamp.

Table S1. Absorption maxima and coefficients of the ring-open and ring-closed isomers, together with the conversion ratios in CH<sub>3</sub>CN from <sup>1</sup>H NMR measurements.

	Absorption maxima (nm) of ring-open isomer	Absorption maxima (nm) of ring-closed isomer	ε of ring-open isomer	ε of ring-closed isomer (Vis region ~666 nm)	ε of ring-closed isomer (UV region ~295 nm)	Conversion ratios from ring-open to ring-closed form
DAE-I	296	316, 382, 666	27835	26563	8692	70%
DAE-BF <sub>4</sub>	296	316, 382, 664	22428	20826	8615	70%
DAE-TFSI	296	316, 382, 666	31177	25474	18037	82%

## Pump probe measurements and calculations of DAE-X and PEO-*stat*-PAGE-DAE-X

### Instrumentation and experimental setup

The kinetics of DAE switching were measured on a home-built pump-probe system. The probe beam was generated by a wide range deuterium, tungsten halogen light source (Ocean Optics DH-mini) coupled into a multimode optical fiber terminated with an output collimator. The visible pump beam was generated by a high-power white LED source (Thorlabs MWWHF2) coupled into a multimode optical fiber terminated with an output collimator. The UV pump source was generated by a Deep UV LED (Thorlabs M300F2) which was positioned to directly illuminate the sample. The probe light was modulated by a shutter (Uniblitz CS25) which could be controlled manually or through a digital output port (National Instruments USB-6009) using LabVIEW. The sample holder allowed for 10x10 mm<sup>2</sup> spectrophotometer cells to be held within, or cast film samples to be held to the front using metal spring clips. Solutions were mixed during measurement using a miniature stirring plate inserted into the sample holder (Starna Cells SCS 1.11). The sample holder was placed into a metal enclosure to prevent exposure to ambient light. The probe beam was directed by a system of lenses into the detector (Ocean Optics Flame-S1-XR spectrometer), which acquired spectra of the probe light. The detector was connected to a PC via USB port. The experiment was controlled by a National Instrument LabVIEW program which collected the probe light spectra, determined sample optical absorption spectra, and controlled pump and probe light sources.

The PEO-*stat*-PAGE-DAE-X were dissolved in dichloroethane (~35 mg/mL). This solution was then spin coated onto precleaned (sonicated in Hellmanex 2% aqueous solution for 30 min, deionized water for 15 min for 2 times, acetone for 15 min and then isopropanol for 15 min and dried with nitrogen) and air-plasma treated (~10 min) quartz substrates at 1000 rpm for 1 min. Film thickness were determined to be approximately 700 nm using profilometry.

### Data interpretation

The instantaneous concentration of ring-open/closed form DAE-X species were calculated using extinction coefficients (Table S1) measured in acetonitrile. The concentrations of closed form species were calculated using the following equation:

$$\frac{[Closed]_t}{[Open]_0} = \frac{A_{670\text{ nm},t}/\epsilon_{closed, 670\text{ nm}}}{A_{300\text{ nm},0}/\epsilon_{open, 300\text{ nm}}}$$

Where  $A_{670\text{ nm},t}$  is the absorbance measured at time  $t$  at 670 nm,  $A_{300\text{ nm},0}$  is the absorbance measured at the start of the experiment at 300 nm.



Solution photoswitching (phthalimide protected DAE-X) (Pro-DAE-X)

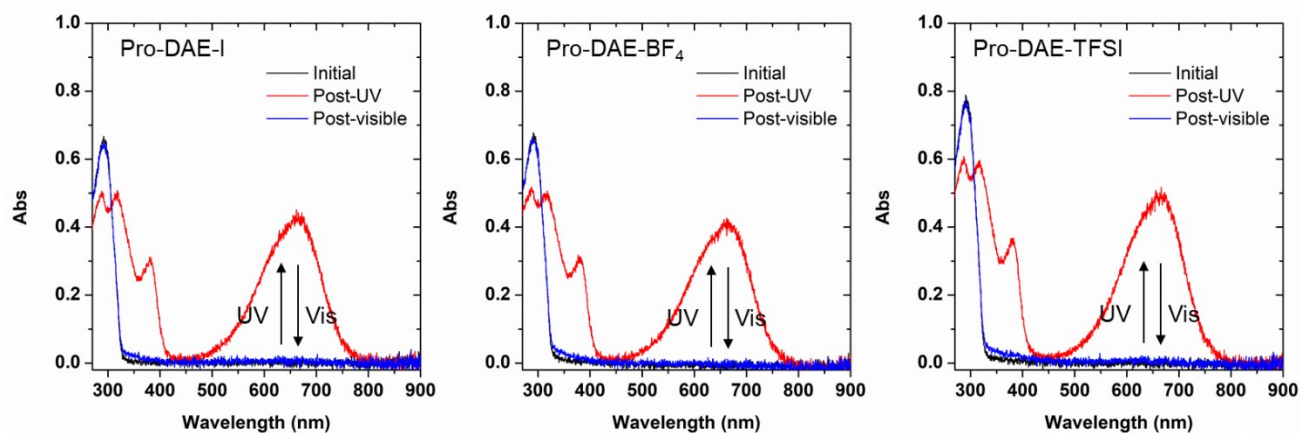


Figure S4. UV-Vis absorption spectra of Pro-DAE-X in  $\text{CH}_3\text{CN}$ . In each case, exposure to visible light returns the spectra to the initial state.

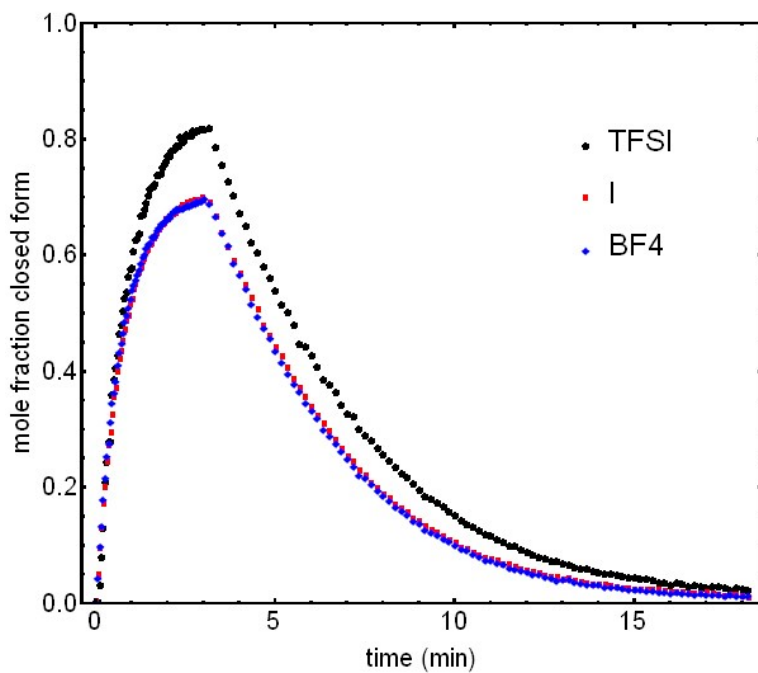


Figure S5. Kinetic traces of Pro-DAE-X in  $\text{CH}_3\text{CN}$  during an initial exposure to 300 nm light followed by exposure to broadband white light with continuous stir. The concentration of the solutions for measurements are approximately  $3 \times 10^{-5}$  mol/L.

**DFT calculation.** The DFT calculation on imidazolium containing DAE cations was carried out by Gaussian 16, in combination of B3LYP/6-311G(d). Frequency and energy (time-dependent DFT, TD-DFT) calculations were performed on the imidazolium-containing DAE cations, with ring-open and ring-closed isomers. To simplify the calculation, an imidazolium unit with a propyl group was introduced to mimic the alkyl chain between the imidazolium unit and the polymer backbone. The +1 charge was introduced to induce positively charged imidazolium unit.

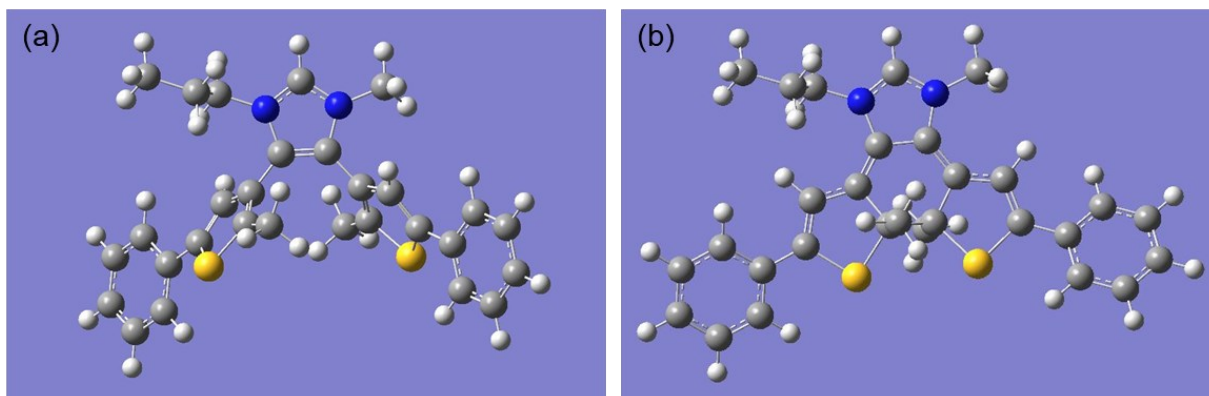


Figure S6. Optimized geometry of imidazolium containing DAE cations, with (a) ring-open and (b) ring-closed isomers.

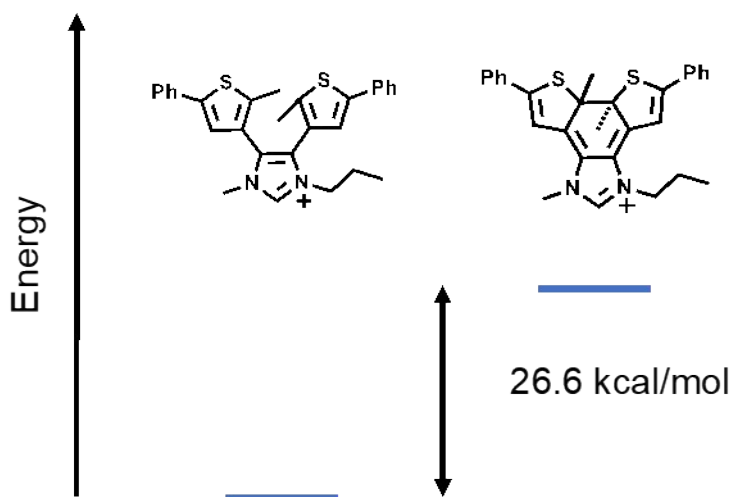


Figure S7. Calculated enthalpy difference of ring-open and closed isomers for imidazolium-containing DAE.

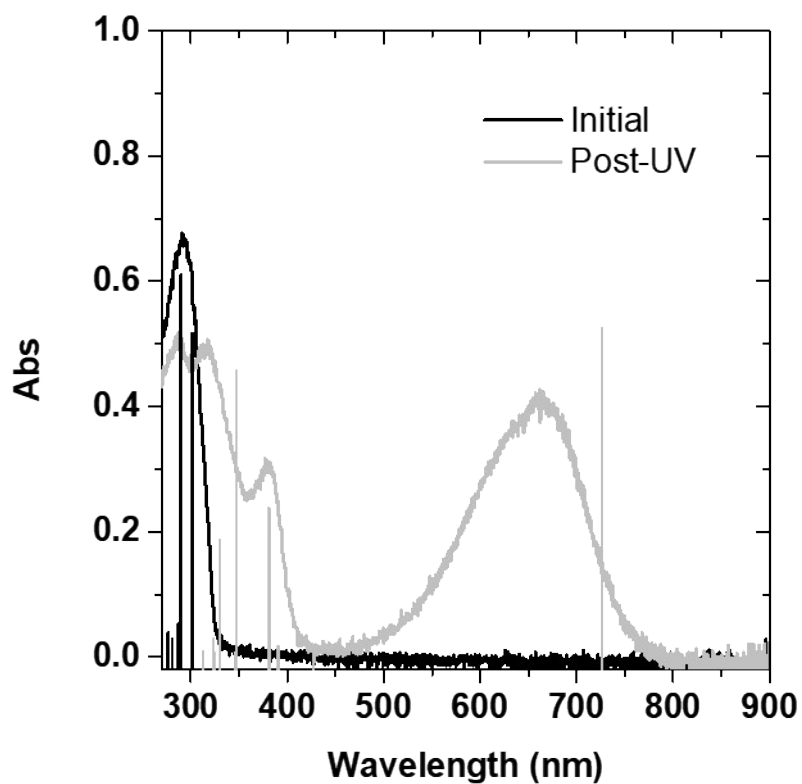


Figure S8. Overlaid experimental UV-vis absorption spectra with the calculated spectra from TD-DFT. Black and gray traces indicate the ring-open and ring-closed isomers, respectively.

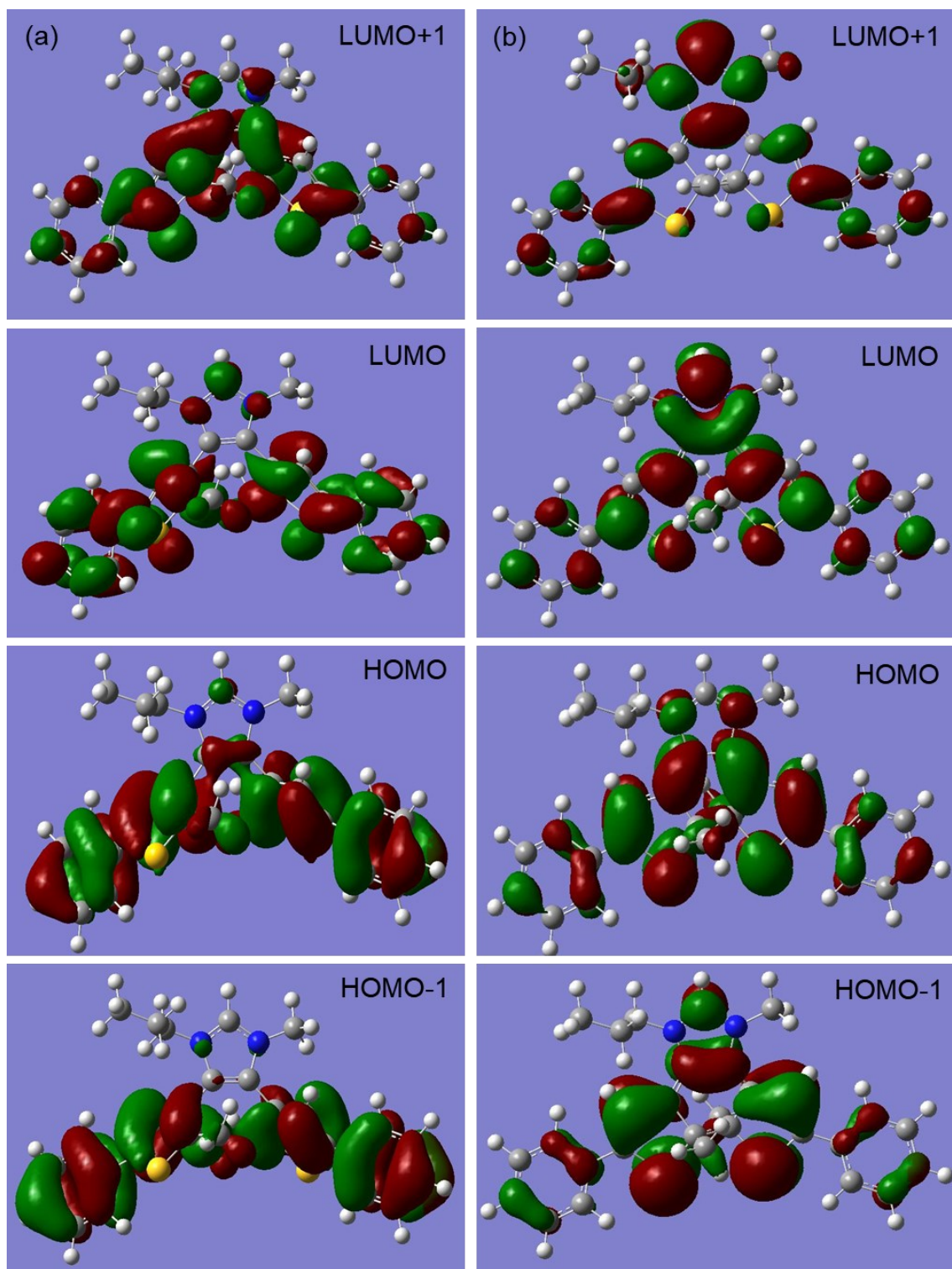


Figure S9. The calculated frontier orbitals of (a) ring-open and (b) ring-closed isomers of imidazolium-containing DAE

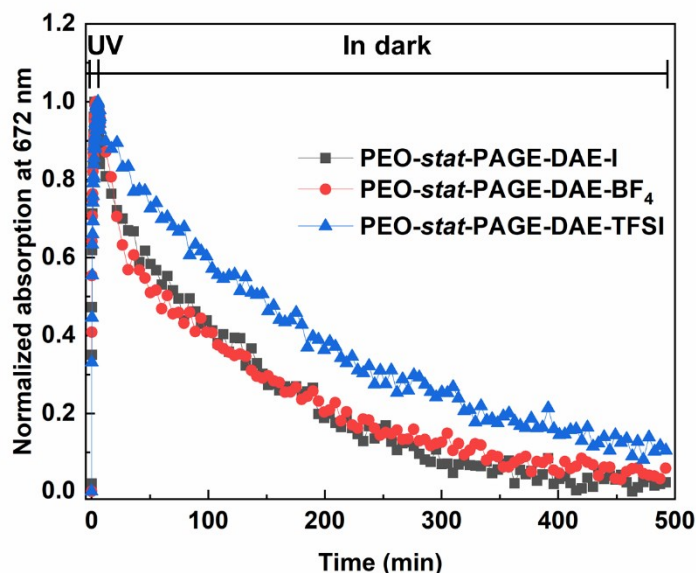


Figure S10. Kinetic traces of PEO-*stat*-PAGE-DAE-X solid films during an initial exposure to 300 nm light followed by in dark condition. Compared with ring-closed to ring-open isomerization by visible light irradiation (finished within 30 min), the thermal back isomerization in dark took a much longer time (greater than 8 h). In addition, the thermal back isomerization rates are PEO-*stat*-PAGE-DAE-I  $\approx$  PEO-*stat*-PAGE-DAE-BF<sub>4</sub> > PEO-*stat*-PAGE-DAE-TFSI.

Table S2. Arrhenius parameters for thermal backward reactions of the ring-closed DAE isomers in polymer films

Samples	$t_{1/2}$ /min at 20 °C	$E_a$ /kJ mol <sup>-1</sup> <sup>a</sup>
PEO- <i>stat</i> -PAGE-DAE-I	74	158 $\pm$ 25
PEO- <i>stat</i> -PAGE-DAE-BF <sub>4</sub>	65	150 $\pm$ 22
PEO- <i>stat</i> -PAGE-DAE-TFSI	147	180 $\pm$ 3

<sup>a</sup>The thermal backward reaction were tracked at 20, 27, 32 °C for  $E_a$  calculation.

To determine the activation energy ( $E_a$ ) of the thermal backward reaction, pump probe measurements of PEO-*stat*-PAGE-DAE-X (I, BF<sub>4</sub>, TFSI) at different temperatures were carried out to extract their rate constant  $k$ . The activation energy of thermal backward reactions of PEO-*stat*-PAGE-DAE-X were calculated by plotting  $\ln k$  versus  $1/T$ , knowing that the slope will be equal to  $-(E_a/R)$  based on the Arrhenius equation.

Compared with DAE molecules in solution, the activation energy of covalently attached DAE in solid polymer film is higher than that in solution (typically around 70-140 kJ mol<sup>-1</sup>).<sup>3,4</sup> It is possible that the more rigid environment of DAE units attached on polymer in solid state leads to higher activation energy than small DAE molecules in solution.

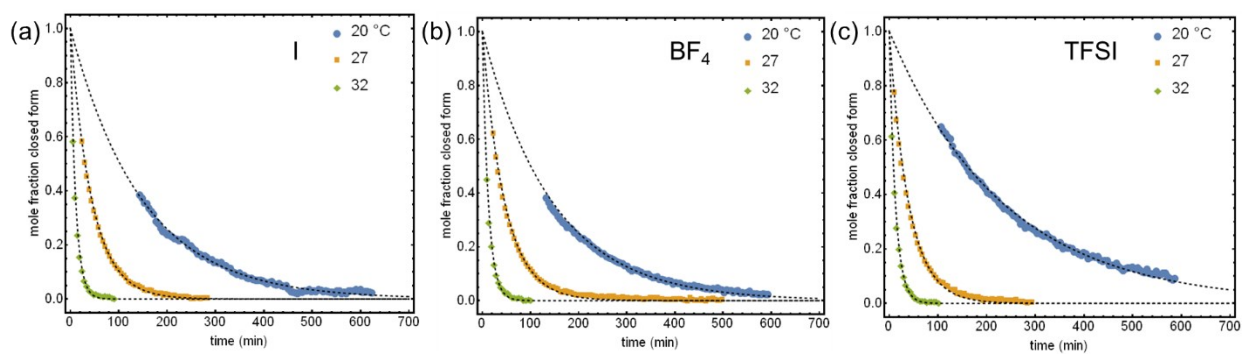


Figure S11. Thermal backward reaction of PEO-*stat*-PAGE-DAE-I (a); BF<sub>4</sub> (b); TFSI (c) in solid film. Absorbance was monitored at ~672 nm of ring-closed isomers.

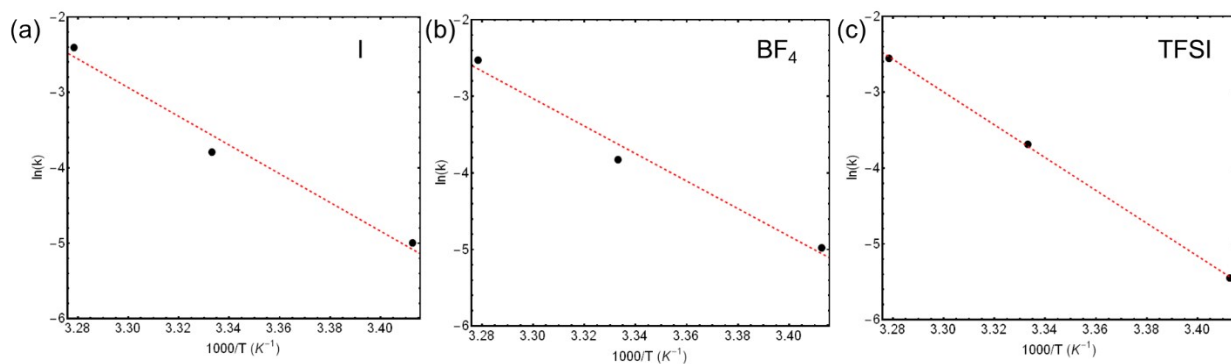


Figure S12. Temperature dependence of the rate constant for the thermal backward reaction of PEO-*stat*-PAGE-DAE-I (a); BF<sub>4</sub> (b); TFSI (c) in solid film.



## Thin film photoswitching

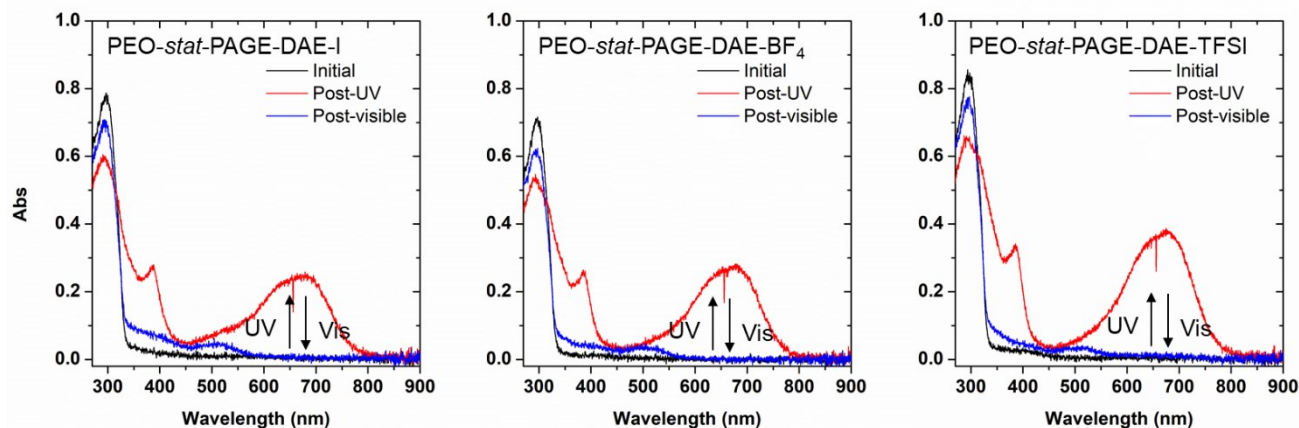


Figure S13. UV-Vis absorption spectra of PEO-*stat*-PAGE-DAE-X thin films. In each case, exposure to visible light returns the spectra to the initial state, with a small residual peak  $\sim 500$  nm, likely corresponding to degradation product.

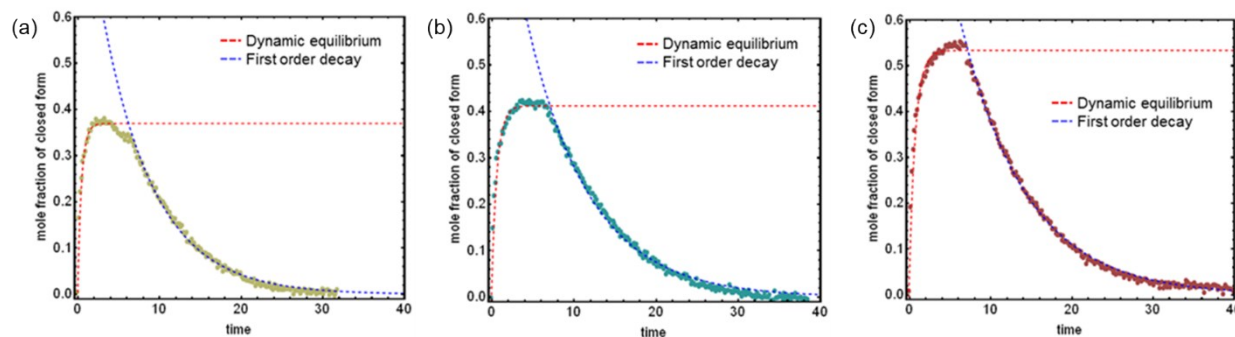


Figure S14. Kinetic traces of (a) PEO-*stat*-PAGE-DAE-I; (b) PEO-*stat*-PAGE-DAE-BF<sub>4</sub>; (c) PEO-*stat*-PAGE-DAE-TFSI thin films during an initial exposure to 300 nm light followed by exposure to broadband white light. The UV exposure was modeled by a first order dynamic equilibrium model, while the white light exposure was modeled with a simple first-order decay.

We suspect that the decreased molar fraction of ring-closed form for PEO-*stat*-PAGE-DAE-I during UV-light irradiation (4-6 min period time) originates from the formation of the annulated isomer byproduct that can form during UV-light irradiation. As shown in Figure 3 and Figure S14a, the DAE-I units reach photostationary state at approximately 2.5 min. Upon continued UV-light irradiation we observe a decrease in the absorbance of ring-closed isomer at 660 nm and an increase of the absorbance at 520 nm from the annulated isomer (Figure S13a). This observation is consistent with the formation of the annulated isomer which is a known decomposition byproduct of DAE based photoswitches.<sup>5</sup>

Table S3. Photoswitching properties of PEO-*stat*-PAGE-DAE-X thin films.

<b>Polymer films</b>	<b>UV (<math>k: \text{min}^{-1}</math>)</b>		<b>White (<math>k: \text{min}^{-1}</math>)</b>
	$k_{\text{open}}$	$k_{\text{close}}$	$k_{\text{open}}$
PEO- <i>stat</i> -PAGE-DAE-I	1.34	0.79	0.157
PEO- <i>stat</i> -PAGE-DAE-BF <sub>4</sub>	0.91	0.64	0.132
PEO- <i>stat</i> -PAGE-DAE-TFSI	0.62	0.71	0.123

### Ionic conductivity measurements

For the bulk ionic conductivity measurement, fully dried polymer samples were cast into 3/16" clean circular indium tin oxide (ITO) substrates top-coated with a 150  $\mu\text{m}$  Kapton spacer. The samples were sealed with clean ITO substrates and characterized with a Biologic SP-200 potentiostat. A sinusoidal voltage with amplitude 50 mV was applied in the frequency range of 1 Hz–1 MHz. The data was converted into dielectric storage and loss, and the ionic conductivities determined from the real component of conductivity at the maximum in  $\tan(\delta)$ .

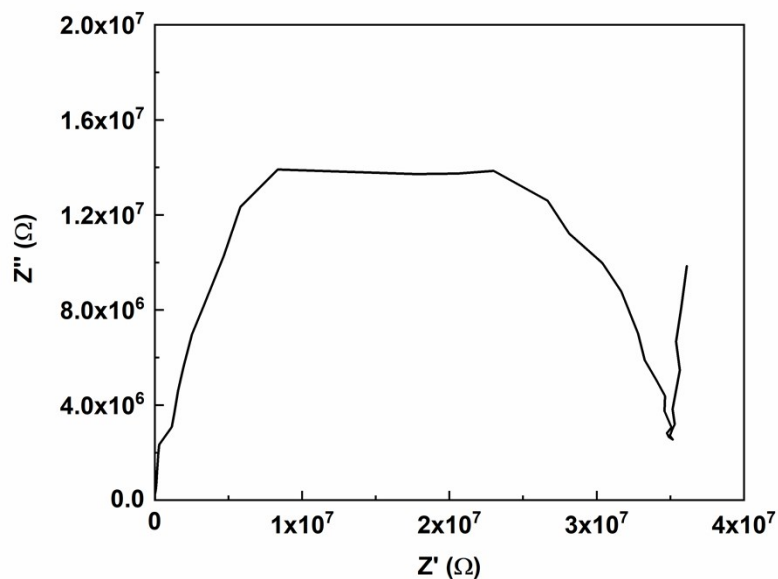


Figure S15. Sample EIS spectra collected for through-plane bulk conductivity measurements.



Table S4. Activation energies calculated for PEO-*stat*-PAGE-DAE-X (I<sup>-</sup>, BF<sub>4</sub><sup>-</sup>, TFSI<sup>-</sup>) by fitting with the Arrhenius Equation and VFT formalism.

	$E_a$ (eV) <sup>a</sup>	$E_a$ (eV) <sup>b</sup>
PEO- <i>stat</i> -PAGE-DAE-I	1.287	0.130
PEO- <i>stat</i> -PAGE-DAE-BF <sub>4</sub>	1.173±0.104 <sup>c</sup>	0.117
PEO- <i>stat</i> -PAGE-DAE-TFSI	1.339	0.123

<sup>a</sup> Calculated activation energies from Arrhenius Equation; <sup>b</sup> Calculated activation energies from VFT formalism; <sup>c</sup> Average value of two measurements. The conductivity measurements were conducted between a temperature range of 30 °C to 70 °C.

Arrhenius Equation:

$$\sigma = \sigma_0 \exp\left(-\frac{E_a}{kT}\right)$$

where  $k$  is Boltzmann's constant ( $8.6173 \times 10^{-5}$  eV/K),  $T$  is the temperature in K,  $E_a$  is an activation energy (in eV), and  $\sigma_0$  is the conductivity prefactor.

VFT formalism:

$$\sigma = A \exp\left(-\frac{B}{(T - T_g + 50)}\right)$$

#### Thin film ionic conductivity measurements

In-plane ionic conductivity measurements of PEO-*stat*-PAGE-DAE-X were performed by spin-coating the polymer onto quartz slides, followed by depositing Au electrodes onto the thin films through evaporation. Specifically, the quartz slides were cleaned by sonication for 5 minutes (each) in soapy water, DI water, acetone and isopropanol, followed by a 5-minute UV/ozone treatment. Gold contacts were thermally evaporated using a shadow mask. Polymer samples in chlorobenzene with a concentration of about 80 mg/ml were spin-coated on the above electrodes for measurements. Conductivity was measured using electrochemical impedance spectroscopy (EIS) on a Biologic SP-200 potentiostat with a sinusoidal 300 mV signal applied over a frequency range of 1 MHz to 80 mHz. All the measurements were conducted in a nitrogen atmosphere glove box at room temperature (about 27 °C to 29 °C). The conductivity was analyzed by fitting to a Randles equivalent circuit and extracting the resistivity from R2–R1 in the circuit diagram seen in Figure S14. Conductivity was then calculated using the dimensions of the sample ( $w = 44 \mu\text{m}$ ,  $l = 1.37 \text{ mm}$  and  $t = 1.15 \mu\text{m}$ ). The UV light source used for the solid film is a Entela Model UVGL-55 Multiband UV-254 NM with 0.16 A current.

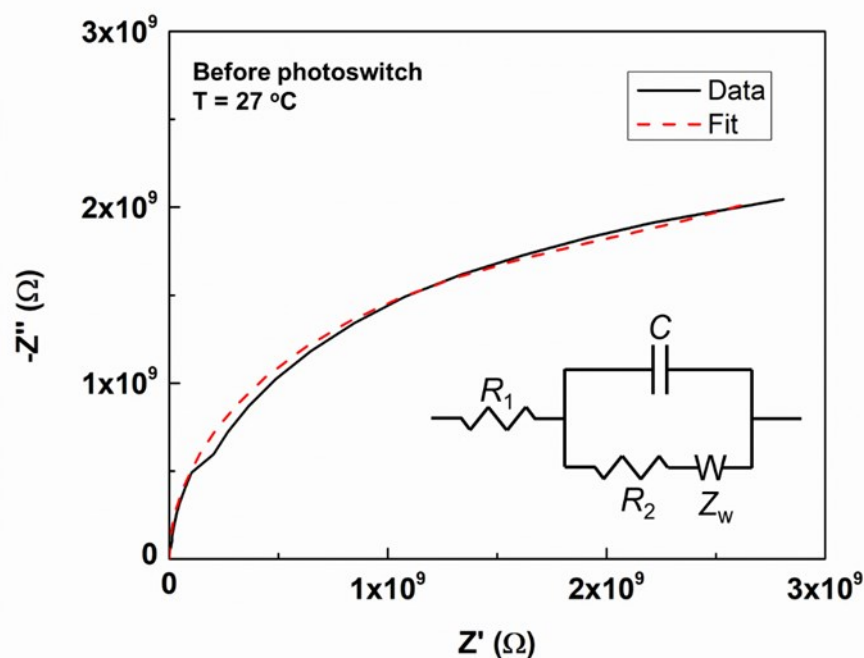


Figure S16. Equivalent circuit and sample EIS spectra collected for in-plane conductivity measurements.

To measure the cycling properties of polymer films with light irradiation, through-plane ionic conductivity measurements of PEO-*stat*-PAGE-DAE-X samples were performed. To improve the conductivity signal, PEO-*stat*-PAGE-DAE-X polymers were mixed with 50 wt% propylene carbonate (plasticizer) in DCM. After removing the solvent and drying under vacuum for approximately 1 h, polymer solutions with concentration of 35 mg/ml (polymer) in 1,2-dichloroethane were prepared for spin-coating on the patterned ITO slide. The ITO slides were cleaned according to general procedure and then the PEO-*stat*-PAGE-DAE-X material was spin-coated on the ITO slides using 1000 rpm for 1 min. To this material gold (Au) electrodes were evaporated on top of the polymer film for conductivity measurements with light irradiation. To minimize the effect of temperature on the conductivity of thin films after light irradiation, light sources were moved away from the films (greater than 8 cm), and measurements were conducted after the films were allowed to cool down to ambient temperature. This took approximately 2 minutes, where the time was determined by the formation of a stable signal.

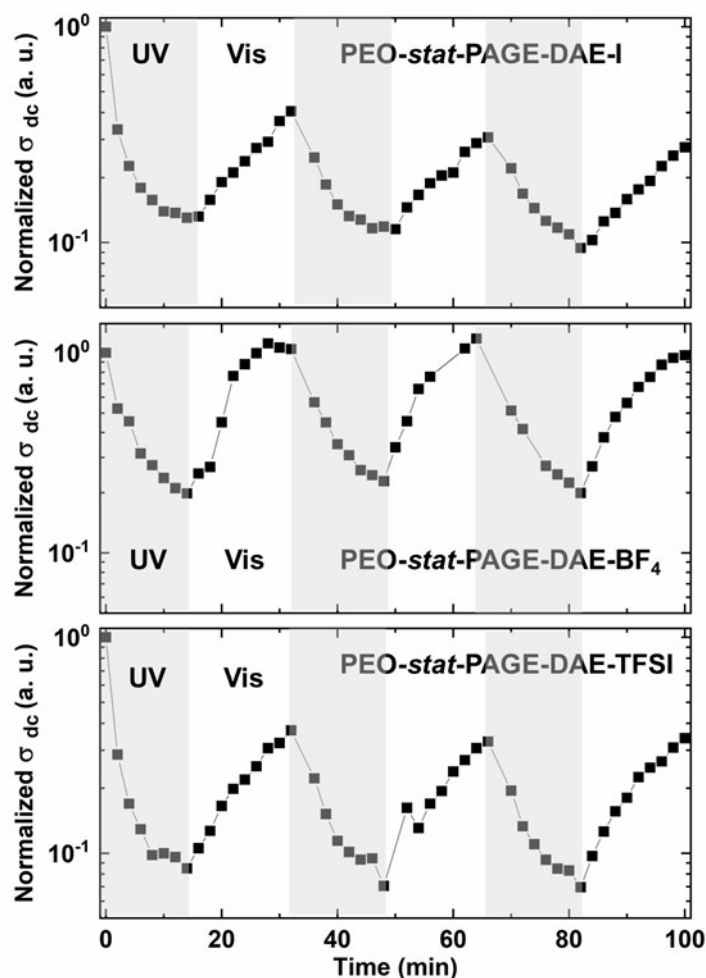


Figure S17. Change in the ionic conductivity of PEO-stat-PAGE-DAE-X films over three cycles of light irradiation.

During the light irradiation process, the generated local Joule heating can have a small effect on the thermal reversion reaction of DAE based photoswitches within the thin films. This effect would be the most pronounced with the DAE-BF<sub>4</sub> group which has the lowest activation energy for the thermal back reaction compared with DAE-I and DAE-TFSI (Table S2). Although further studies are needed, this could provide a rational for the more facile recovery of conductivity with visible-light irradiation.

**$T_g$ s of PEO-*stat*-PAGE-DAE-BF<sub>4</sub> before and after irradiation**

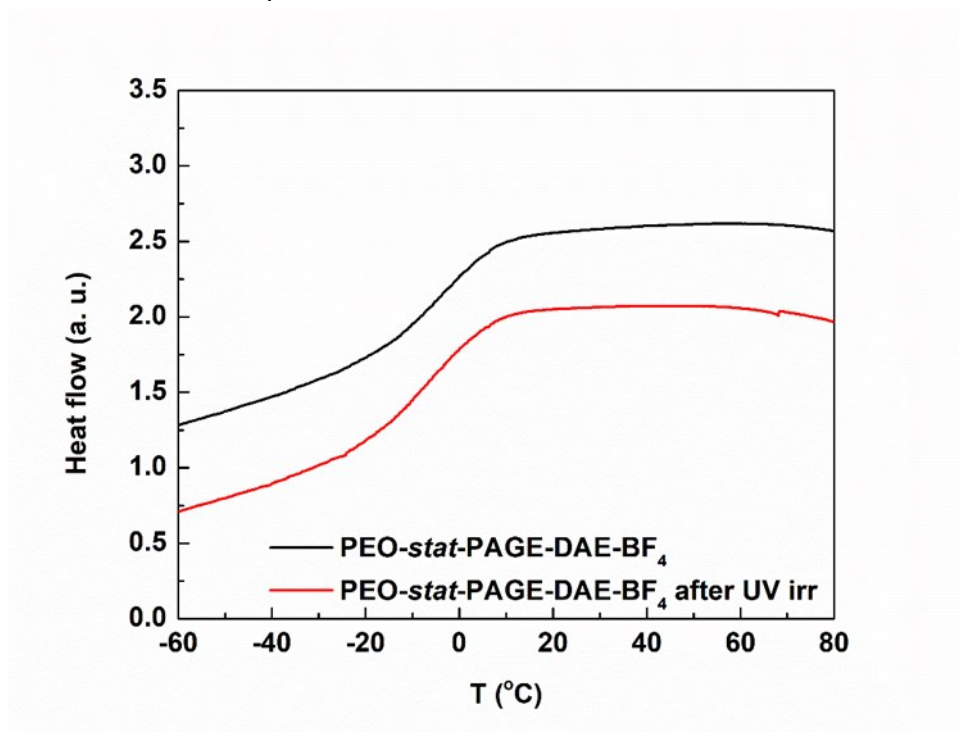
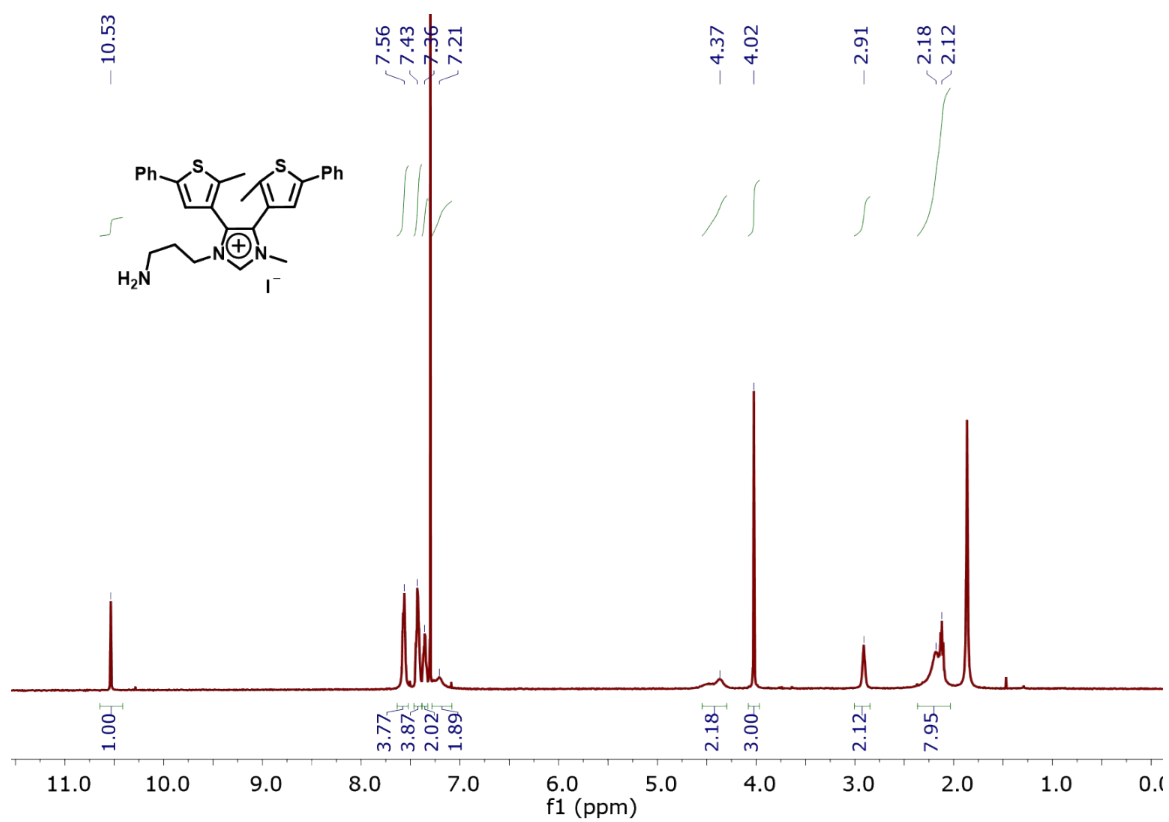
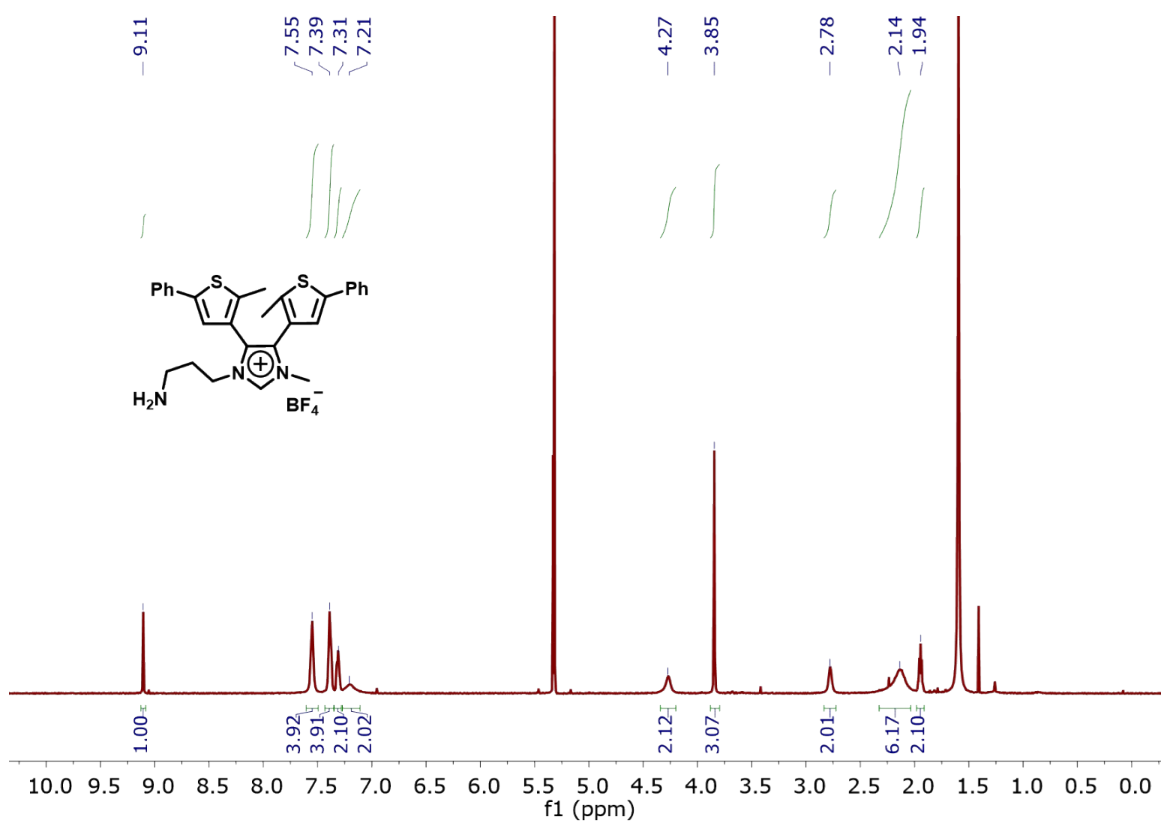
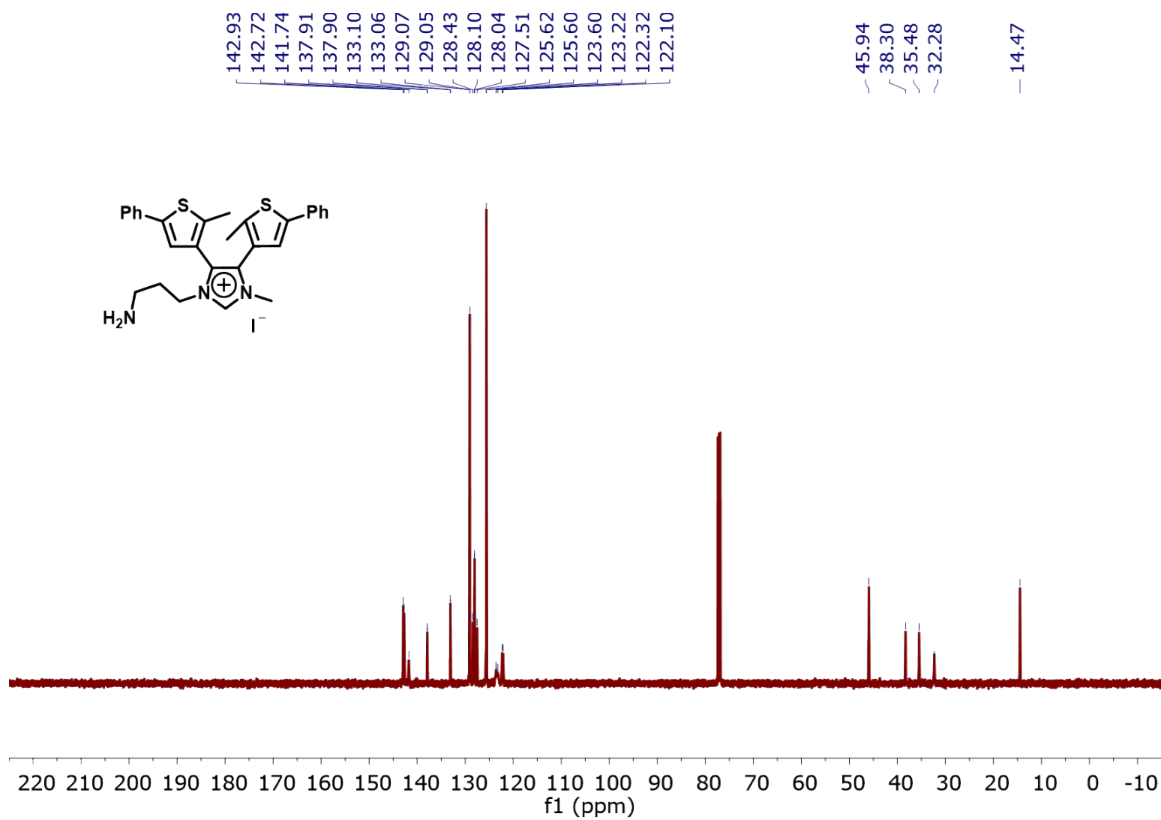
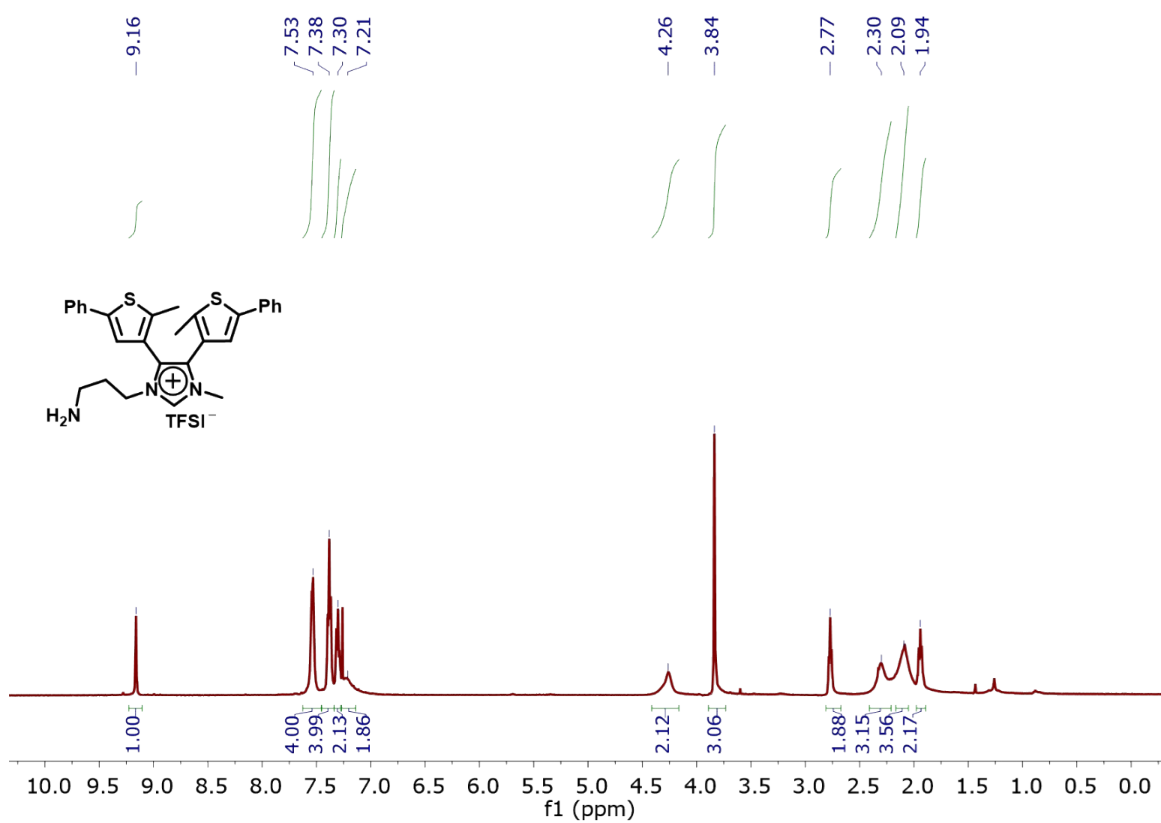
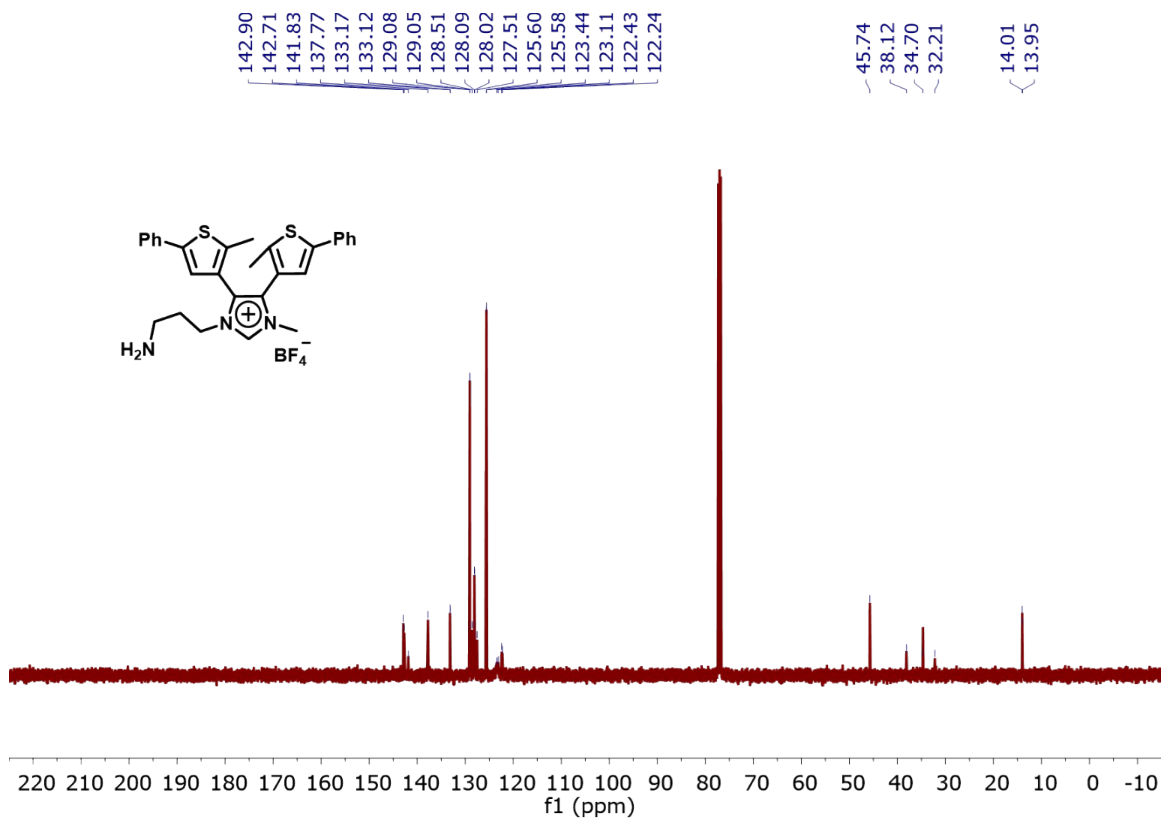


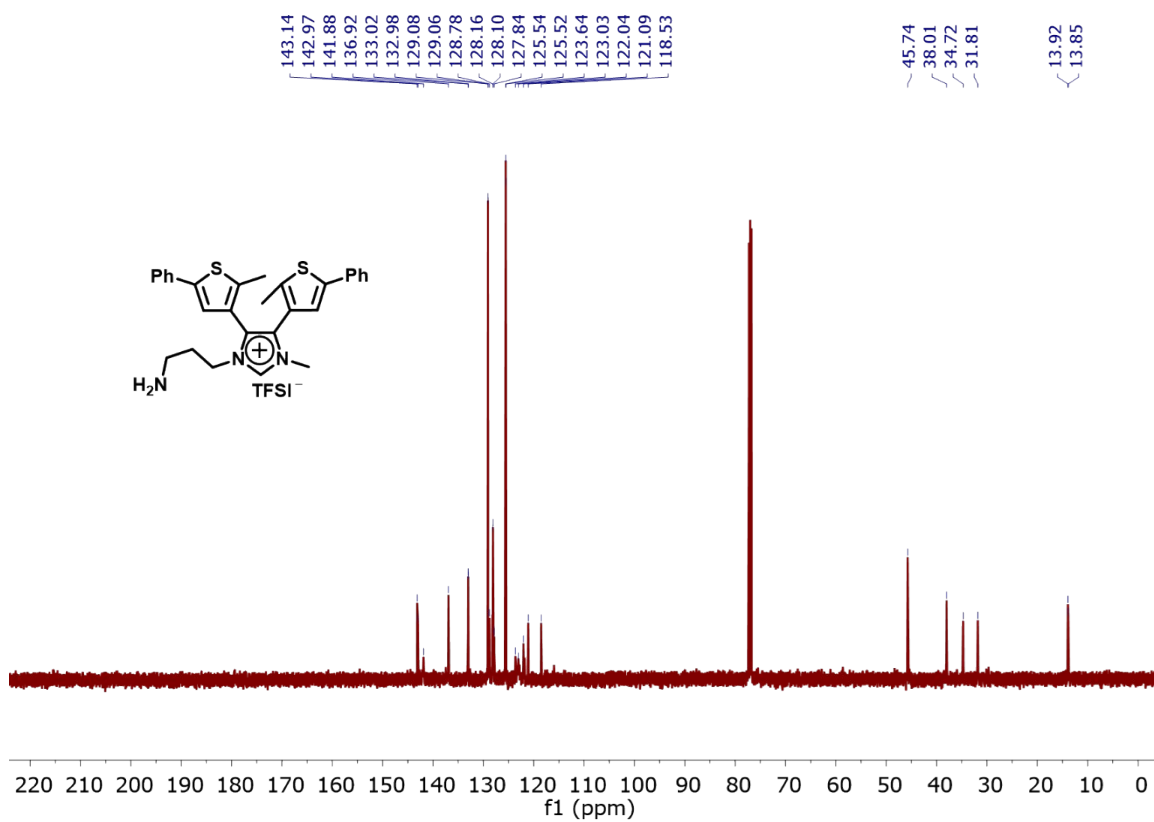
Figure S18. Differential scanning calorimetry of PEO-*stat*-PAGE-DAE-BF<sub>4</sub> for determination of the  $T_g$  before and after UV light irradiation. Data collected on second heating at 20 °C/min.

# $^1\text{H}$ NMR and $^{13}\text{C}$ NMR spectra

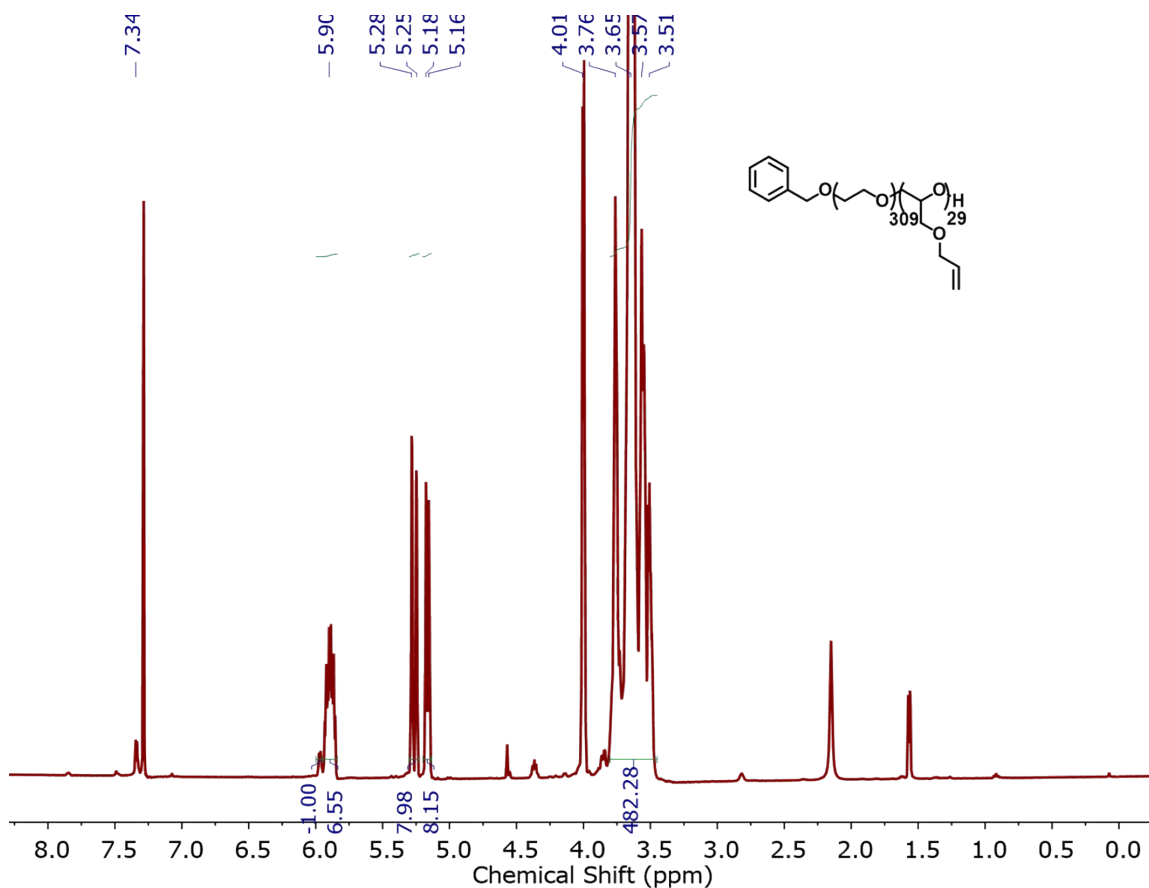












## References

- (1) Nie, H.; Schauser, N. S.; Dolinski, N. D.; Hu, J.; Hawker, C. J.; Segalman, R. A.; Read de Alaniz, J., Light-Controllable Ionic Conductivity in a Polymeric Ionic Liquid. *Angew. Chem. Int. Ed.* 2020, 59, 5123–5128.
- (2) Lee, B. F.; Wolffs, M.; Delaney, K. T.; Sprafke, J. K.; Leibfarth, F. A.; Hawker, C. J.; Lynd, N. A., Reactivity Ratios and Mechanistic Insight for Anionic Ring-Opening Copolymerization of Epoxides. *Macromolecules* 2012, 45, 3722–3731.
- (3) Gurke, J., Quick, M., Ernsting, N. P., Hecht, S. Acid-catalysed thermal cycloreversion of a diarylethene: a potential way for triggered release of stored light energy? *Chem. Commun.*, 2017, 53, 2150-2154.
- (4) Shoji, H., Kitagawa, D., Kobatake, S., Alkyl substituent effects in photochemical and thermal reactions of photochromic thiophene-S,S-dioxidized diarylethenes, *New J. Chem.*, 2014, 38, 933-943.
- (5) Herder, M., Schmidt B. M., Grubert, L., Pätzelt, M., Schwarz, J., Hecht S., Improving the Fatigue Resistance of Diarylethene Switches, *J. Am. Chem. Soc.* 2015, 137, 2738–2747.